Controlled Growth of ZnO Nanowires and Their Optical Properties**

By *Peidong Yang*,* *Haoquan Yan*, *Samuel Mao*, *Richard Russo*, *Justin Johnson*, *Richard Saykally*, *Nathan Morris*, *Johnny Pham*, *Rongrui He*, and *Heon-Jin Choi*

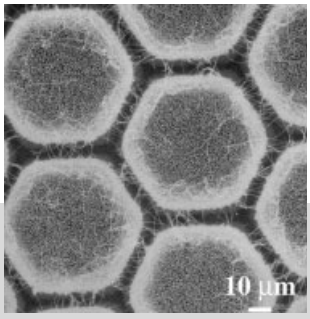

This article surveys recent developments in the rational synthesis of single-crystalline zinc oxide nanowires and their unique optical properties. The growth of ZnO nanowires was carried out in a simple chemical vapor transport and condensation (CVTC) system. Based on our fundamental understanding of the vapor–liquid–solid (VLS) nanowire growth mechanism, different levels of growth controls (including positional, orientational, diameter, and density control) have been achieved. Power-dependent emission has been examined and lasing action was observed in these ZnO nanowires when the excitation intensity exceeds a threshold (~40 kW cm^{-2}). These short-wavelength nanolasers operate at room temperature and the areal density of these nanolasers on substrate readily reaches 1 × 10^{10} cm^{-2}. The observation of lasing action in these nanowire arrays without any fabricated mirrors indicates these single-crystalline, well-facetted nanowires can function as self-contained optical resonance cavities. This argument is further supported by our recent near-field scanning optical microscopy (NSOM) studies on single nanowires.

1. Introduction

Nanoscale one-dimensional (1D) materials have stimulated great interest due to their importance in basic scientific research and potential technological applications.[1–3] Other than carbon nanotubes, 1D nanostructures such as nanowires or quantum wires are ideal systems for investigating the dependence of electrical transport, optical and mechanical properties on size and dimensionality. They are expected to play an important role as both interconnects and functional components in the fabrication of nanoscale electronic and optoelectronic devices. Many unique and fascinating properties have already been proposed or demonstrated for this class of materials, such as superior mechanical toughness,[4] higher luminescence efficiency,[5] enhancement of thermoelectric figure of merit,[6] and a lowered lasing threshold.[7] Previously, nanowires with different compositions have been explored using various methods, including vapor phase transport processes,[8–10] chemical vapor deposition,[11,12] arc-discharge,[13] laser ablation,[12,14] and solution[5,15] and template-based methods.[16,17] While a large part of these works has been focused on semiconductor systems such as Si,[1,12] Ge,[8] GaN,[9] and GaAs,[1,11] it is only very recently that 1D oxide nanostructures have started to emerge as very promising nanoscale building blocks because of their interesting properties, diverse functionalities, surface cleanness, and chemical/thermal stability.[2,3,7,10,18,19]

On the other hand, the interest in developing short-wavelength semiconductor lasers has culminated in the realization of room-temperature green–blue diode laser structures with ZnSe and $In_xGa_{1-x}N$ as the active layers.[20–22] Zinc oxide (ZnO) is a wide bandgap (3.37 eV) semiconductor, for which ultraviolet lasing action has been reported in disordered particles and thin films.[23–25] For wide bandgap semiconductors, a high carrier concentration is usually required in order to reach an optical gain that is high enough for lasing action in an electron–hole plasma (EHP) process.[26] Such an EHP mechanism, which is common for conventional laser diode operation, typically requires high lasing thresholds. As an alternative to EHP, excitonic recombination in semiconductors is a more efficient radiative process and can facilitate low-threshold stimulated

[*] Prof. P. Yang, H. Yan, J. Johnson, Prof. R. Saykally, N. Morris, J. Pham, R. He, Dr. H.-J. Choi
Department of Chemistry, University of California
Berkeley, CA 94720 (USA)
E-mail: pyang@cchem.berkeley.edu
Dr. S. Mao, Dr. R. Russo
Environmental Energy Technology Division
Lawrence Berkeley National Laboratory
Berkeley, CA 94720 (USA)

[**] This work was supported by the Camille and Henry Dreyfus Foundation, 3M Corporation, the National Science Foundation, and the University of California, Berkeley. P. Y. is an Alfred P. Sloan Research Fellow. Work at the Lawrence Berkeley National Laboratory was supported by the Office of Science, Basic Energy Sciences, Division of Materials Science of the US Department of Energy. We thank the National Center for Electron Microscopy for the use of their facilities.

 © WILEY-VCH Verlag GmbH, D-69469 Weinheim, 2002 1616-301X/02/0505-0323 $ 17.50+.50/0

emission.[27,28] To achieve efficient excitonic laser action at room temperature, the binding energy of the exciton (E_{ex}^{b}) must be larger than the thermal energy at room temperature (26 meV). In this regard, ZnO is a good candidate for room-temperature UV lasing as its exciton binding energy is approximately 60 meV, significantly larger than that of ZnSe (22 meV) and GaN (25 meV).

Nanostructures are expected to further lower the lasing threshold because quantum effects will result in a substantial density of states at the band edges and enhance radiative recombination due to carrier confinement. The use of semiconductor quantum well structures as low-threshold optical gain media represents a significant advancement in semiconductor laser technology.[29] Light emission from semiconductor nanowhiskers has been reported in GaAs and GaP systems.[30,31] Stimulated emission and optical gain have also been demonstrated recently in Si and CdSe nanoclusters and their ensembles.[32,33] In light of these considerations, ZnO nanowires are considered an interesting system to examine and ascertain their optical properties as a function of size and dimensionality.[7,10,34–36]

Recently, we developed a simple vapor transport and condensation (CVTC) process for the synthesis of ZnO nanowires via the vapor–liquid–solid (VLS) mechanism.[7,8,10] In order to fully exploit the interesting optical properties of these nanowires, we have achieved several important structural control capabilities, namely, orientation, position, and diameter control. In this article, we provide a full account of this simple vapor transport process developed in our laboratory for the synthesis of ZnO nanowires and their structure–property characterization. Grown in a preferred <0001> direction, these wide bandgap semiconductor nanowires form natural laser cavities with diameters varying from 20 to 150 nm and lengths up to 40 μm. Under optical excitation, surface-emitting lasing action was observed at a near UV wavelength of 385 nm with an emission line width <0.3 nm. The power-dependent lasing spectrum indicates the threshold of ~40 kW cm^{-2}, which is much lower than the values reported for ZnO crystals and thin films (~300 kW cm^{-2}). These short-wavelength nanolasers could have myriad applications, including optical computing, information storage, and nanoanalysis.

2. Synthesis and Characterization of ZnO Nanowires

A schematic illustration of the chemical vapor transport and condensation (CVTC) system is shown in Figure 1. Single-crystalline silicon and sapphire of different orientations were used as substrates for the ZnO nanowire growth. The substrates were coated with a layer of Au thin film using a thermal evaporator with a quartz crystal thickness monitor to ensure an exact

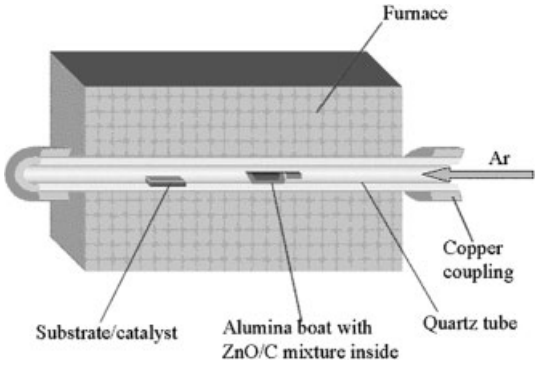

Fig. 1. Schematic illustration of the chemical vapor transport and condensation experimental set-up for ZnO nanowire growth.

Au film thickness. Equal amounts of ZnO powder and graphite powder were ground together and transferred to an alumina boat. The Au-coated substrates and the alumina boat were placed into a small quartz tube. The substrates were typically placed ~5–10 cm from the center of the boat. This quartz tube was then placed inside a furnace quartz tube, with the center of the alumina boat positioned at the center of the furnace and the substrates placed downstream of an argon flow. The temperature of the furnace was ramped to ~800–1000 °C at a rate of ~50–100 °C min^{-1} and typically kept at that temperature for ~5–30 min under a constant flow of argon (~20–25 sccm). After the furnace was cooled to room temperature, light or dark gray material was found on the surface of the substrates. For the growth of ZnO nanowires using Au nanoclusters, spin-coating was used to disperse uniform Au colloids on the substrates.

Peidong Yang is an assistant professor in the chemistry department, University of California, Berkeley. He received a B.S. degree in chemistry from the University of Science and Technology of China in 1993, and a Ph.D. degree in chemistry from Harvard University in 1997. After two years as a postdoc at the University of California, Santa Barbara, he joined the University of California, Berkeley as assistant professor in 1999. His research interests include rational synthesis, assembly, and novel properties (optoelectronic, thermoelectrical, and chemical properties) of one-dimensional nanostructures, and methodology for nano–micro–macro structural interfacing.

© WILEY-VCH Verlag GmbH, D-69469 Weinheim, 2002
1616-301X/02/0505-0324 $ 17.50+.50/0

ADVANCED FUNCTIONAL MATERIALS

Although the VLS crystal growth mechanism has been widely used for semiconductor nanowire growth,[1–3,8] oxide nanowire growth through the VLS mechanism could be complicated by the presence of oxygen. In our studies, the process involves the reduction of ZnO powder by carbon to form Zn and CO/CO_2 vapor in the high-temperature zone. The Zn vapor is transported and reacted with the Au solvent on substrates located downstream at a lower temperature to form alloy droplets (Fig. 2). As the droplets become supersaturated, crystalline ZnO nanowires are formed, possibly by the reaction between Zn and CO/CO_2 in the low temperature zone. The presence of a small amount of CO/CO_2 is not expected to significantly change the Au–Zn phase diagram, meantime the gas mixture acts as the oxygen source during ZnO nanowire growth. Control experiments without graphite addition in the starting materials produce essentially nothing on the Au-coated substrates, which indicates the importance of Zn vapor generated by the carbothermal reduction of ZnO.

Figure 3 shows a typical scanning electron microscopy (SEM) image of ZnO nanowires grown on a silicon substrate. The diameters of the nanowires normally range from 20–120 nm and their lengths are 5–20 μm. X-ray diffraction (XRD) patterns of ZnO nanowires were taken to examine the crystal structure of the nanowires. All samples gave similar XRD patterns, indicating the high crystallinity of nanowires. Figure 4 shows a typical XRD pattern of these ZnO nanowires. The diffraction peaks can be readily indexed to a hexagonal structure with cell constants of $a = 3.24$ Å and $c = 5.19$ Å.

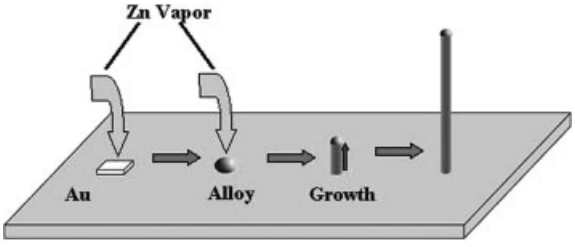

Fig. 2. Schematic representation of ZnO nanowire growth mechanism.

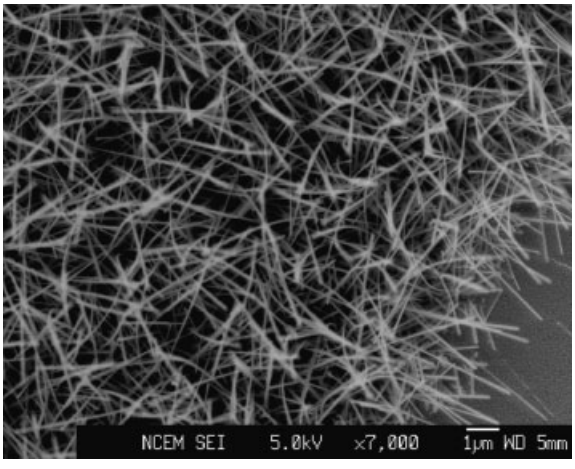

Fig. 3. Scanning electron microscopy images of ZnO nanowires grown on Si(100) substrate.

Additional structural characterization was carried out using transmission electron microscopy (TEM). Figure 5A is a TEM image of a thin nanowire with an alloy tip. The presence of the alloy tip is a clear indication of the VLS growth mechanism. Figure 5B shows a high-resolution TEM image of a single ZnO nanowire. The spacing of 2.56 ± 0.05 Å between adjacent lattice planes corresponds to the distance between two (0002) crystal planes, confirming <0001> as the preferred growth direction for ZnO nanowires.

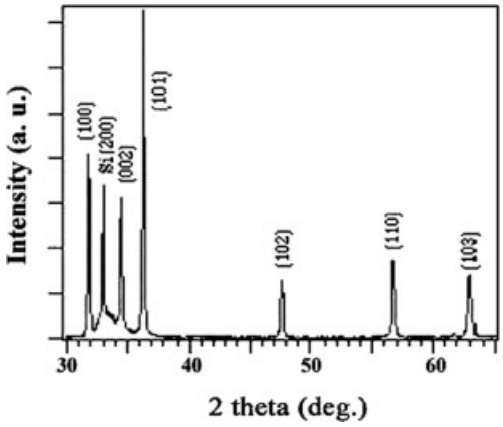

Fig. 4. XRD pattern of ZnO nanowires on silicon substrate.

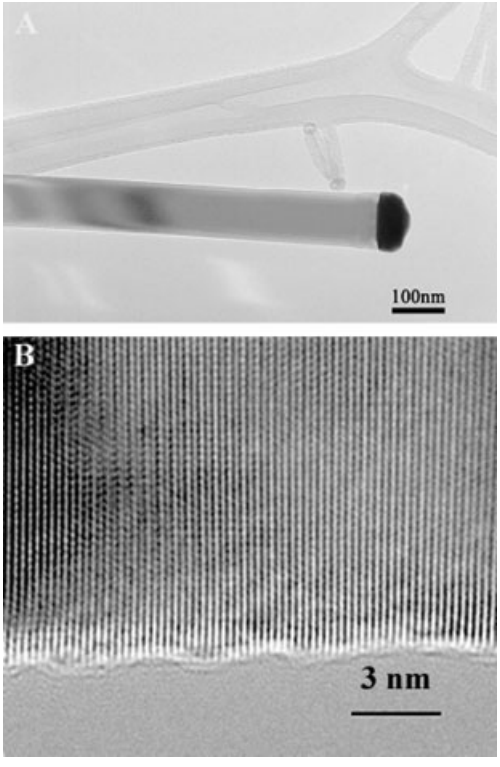

Fig. 5. A) TEM image of a ZnO nanowire with an alloy droplet on its tip. B) High-resolution transmission electron microscopy image of an individual ZnO nanowire showing its <0001> growth direction. Reprinted with permission from [7]. Copyright American Association for the Advancement of Science, 2001.

 © WILEY-VCH Verlag GmbH, D-69469 Weinheim, 2002 1616-301X/02/0505-0325 $ 17.50+.50/0

3. Controlled Growth of ZnO Nanowires

3.1. Control of Orientation

Controlling the growth orientation is important for many of the proposed application of nanowires. By applying the conventional epitaxial crystal growth technique to this VLS process, it is possible to achieve precise orientational control during nanowire growth. This technique, vapor–liquid–solid epitaxy (VLSE), is particularly powerful for the controlled synthesis of nanowire arrays.

Nanowires generally have preferred growth directions. For example, Si nanowires prefer to grow along the <111> direction, while ZnO nanowires prefer to grow along the <001> direction. One strategy to grow vertically aligned nanowires is to properly select the substrate and to control the reaction conditions, so that the nanowires grow epitaxially on the substrate. For example, sapphire is an ideal substrate with lattice constant a = 4.75 Å and c = 12.94 Å. The c surface of sapphire is composed of alternate layers of six-fold symmetric oxygen and threefold symmetric Al atoms, while in the wurtzite structure of ZnO, both O and Zn are six-fold symmetric about the ZnO c-axis. Since the ZnO a-axis and the sapphire c-axis are related almost exactly by a factor of 4 (mismatch less than 0.08 % at room temperature), ZnO nanowires can grow epitaxially from the (110) plane of sapphire (Fig. 6A). Figure 6B shows the growth of ZnO nanowires on an a-plane (110) sapphire substrate. Their diameters range from 40–120 nm and lengths can be adjusted between 2 and 10 μm. They are grown vertically from the substrate, as one can expect from the epitaxial growth. The hexagonal end surface of the nanowires can be readily seen in Figure 6C. This type of nanowire array growth can also be achieved using MgO(111) as substrate. Figure 7 shows a typical XRD pattern recorded on these ZnO nanowire arrays. Only (00*l*) diffraction peaks were observed, indicating excellent (001) orientation/alignment of the nanowires on a large area of the substrate. Previously, InAs nanowhiskers have been oriented on Si substrate using a fairly complicated metal–organic vapor-phase epitaxy technique.[31]

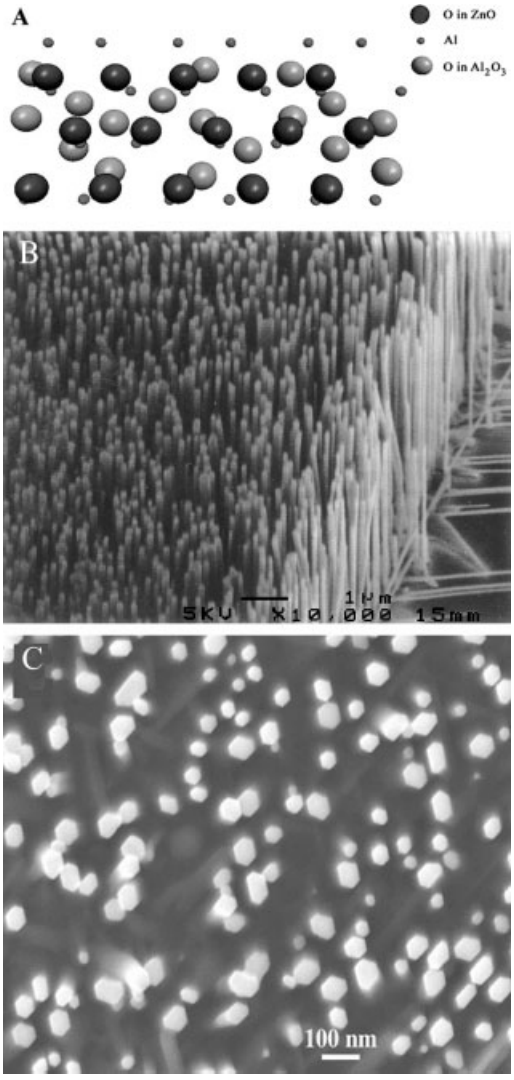

Fig. 6. The epitaxial growth of ZnO nanowires on a-plane (110) sapphire can be readily seen by examination of the crystal structures of ZnO and sapphire (a = 0.4754 nm, c = 1.299 nm). A) Schematic illustration of ZnO ab-plane overlapping with the underlying (110) plane of sapphire substrate. B,C) Arrays of ZnO nanowires grown on a-plane sapphire substrate.

3.2. Control of Position

It is apparent from the VLS nanowire growth mechanism that the positions of the nanowires can be controlled by the initial positions of Au clusters or thin films. Various lithographical techniques, for example, soft lithography, e-beam lithography, and photolithography, can be used to create patterns of Au thin films for subsequent semiconductor nanowire growth.[2,3] SEM studies (Fig. 8) reveal extensive growth of fine, long, and flexible ZnO nanowires from the edges of a hexagonally patterned Au thin film. The wire growth conforms to the hexagonal Au pattern with high fidelity. Most of the wires actually bridge the neighboring metal hexagons and form an intricate network. Figure 8B shows an SEM image of the same sample at a higher magnification to reveal more detail. The nanowires at the edge have a diameter of about 50–200 nm, and can be as long as over 50 μm.

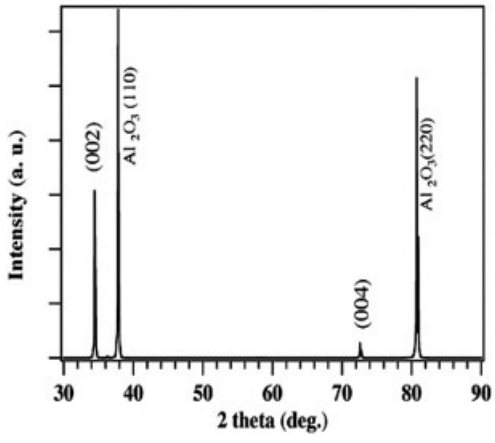

Fig. 7. XRD pattern of ZnO nanowires on sapphire substrate. Reprinted with permission from [7]. Copyright American Association for the Advancement of Science, 2001.

© WILEY-VCH Verlag GmbH, D-69469 Weinheim, 2002
1616-301X/02/0505-0326 $ 17.50+.50/0

ADVANCED FUNCTIONAL MATERIALS

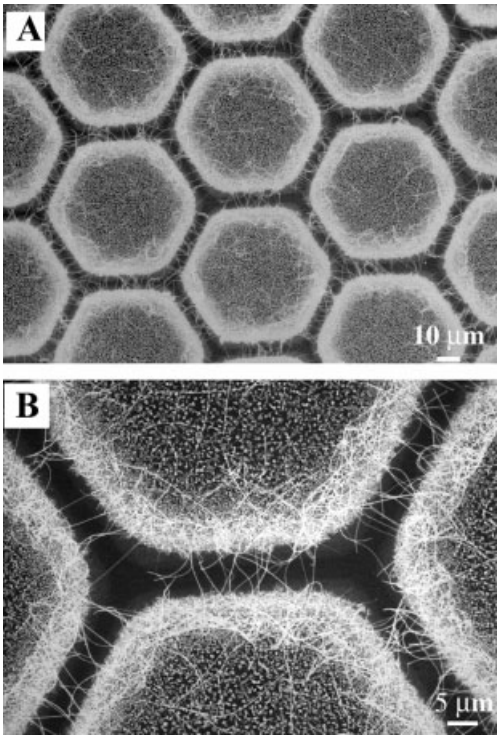

Fig. 8. SEM images of a patterned ZnO nanowire network on Si substrate.

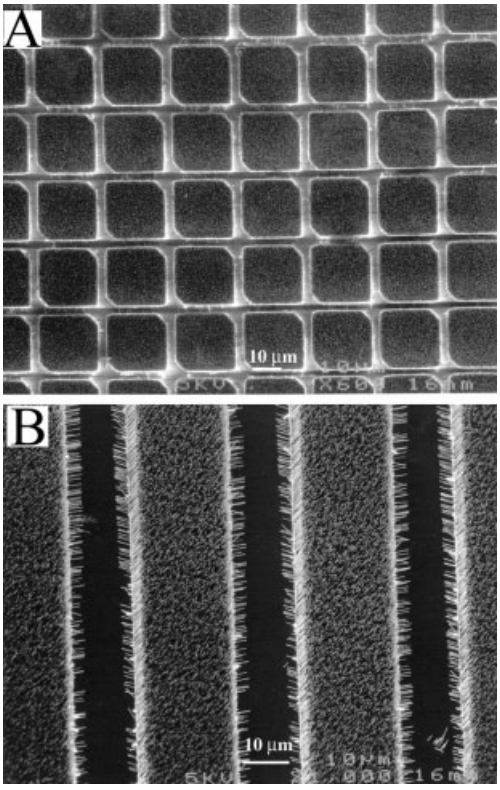

Fig. 9. SEM images of epitaxial growth of line- and square-patterned ZnO nanowires on *a*-plane sapphire substrate.

Figure 9 shows the SEM images of ZnO nanowires grown from the line and square Au patterns on *a*-plane sapphire substrate. Selective epitaxial nanowire growth can readily be seen. It is clear that nanowires grow vertically only from the region that is coated with Au and form designed patterns of ZnO nanowire arrays.

In addition to this positional control, it is further possible to control the nanowire areal density by modifying the thin-film thickness or using solution-made Au clusters. By dispersing a different amount/density of Au clusters on the sapphire substrate, it is possible to obtain nanowire arrays with different densities (Fig. 10). We can now readily synthesize, for example, ZnO nanowire arrays with an areal density spanning 10^6–10^{10} cm^{-2}.

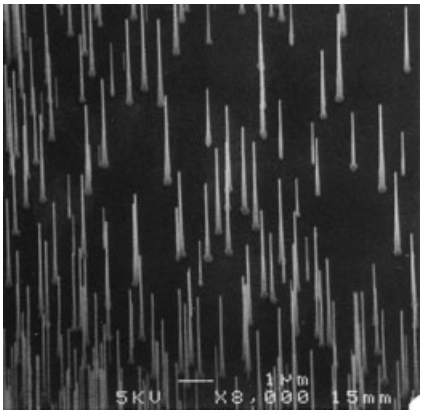

Fig. 10. ZnO nanowire arrays on sapphire substrate with low areal density.

3.3. Control of Diameter

In an effort to grow ZnO nanowires with controllable diameters, substrates coated with Au of different thickness were used. The idea is based on a possible direct relationship between the size of the solvent particles and the resulting diameters of the nanowires. Smaller Au droplets, formed in the heating process during the reaction, should favor the growth of thinner wires. As the thickness of the Au thin film decreases, the width of the wires also decreases. For example, the average diameters of ZnO nanowires grown on *a*-plane sapphire substrates at 900 °C for 5 min are 88, 110, and 150 nm, respectively, when Au thin films of 0.5, 1, and 3 nm thick are used. The smallest diameter of ZnO nanowires we have achieved by using Au thin films is about 40 nm.

In addition, we can also use uniformly distributed Au clusters as solvent to control the widths of the nanowires. The Au nanoclusters were dispersed on silicon substrates or within mesoporous silica films to minimize possible particle aggregation. For example, the average diameters of ZnO nanowires are 35, 46, and 54 nm, respectively, when Au clusters of 5, 10, and 15 nm sizes are used. Compared with the results obtained using a Au thin film, Au clusters produce wires with much thinner widths—as thin as 20 nm. That can be attributed to the fact that when Au thin film melts at high temperature to form Au droplets, there is a thermodynamic limit to the minimum radius of the metal liquid clusters at high temperature, $R_{min} = 2\sigma_{LV}V_L/RT\ln s$, where σ_{LV} is the liquid–vapor surface free energy, V_L is the molar volume of liquid, and s is the vapor phase supersaturation.[1–3]

 © WILEY-VCH Verlag GmbH, D-69469 Weinheim, 2002 1616-301X/02/0505-0327 $ 17.50+.50/0

3.4. Control of Morphology

By using different vapor sources, it was recently discovered that certain superstructures of the nanowires readily form. For example, when Zn powder was used as vapor source, a large yield of comb-like structures made of ZnO nanowires can be synthesized (Fig. 11). These nanowires have uniform diameters and are uniformly distributed on the side of the stem. Other superstructures, such as tetra-pods and tapered nanowires, can also be formed under different evaporation conditions. These different superstructures may have interesting physical properties, and particularly optical properties.

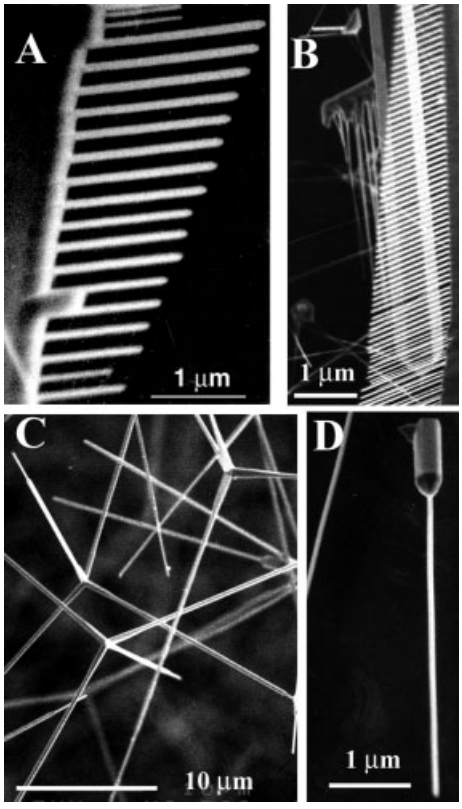

Fig. 11. Different morphologies and superstructures based on ZnO nanowires synthesized using Zn as the vapor source.

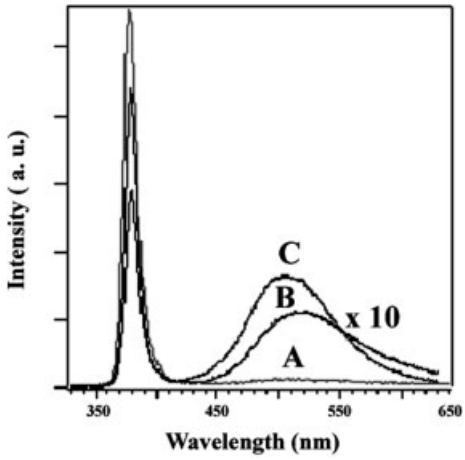

Fig. 12. Photoluminescence spectra of ZnO nanowires of different diameter recorded at room temperature. Spectra A, B, C correspond to nanowires with average diameters of 100, 50, and 25 nm, respectively.

wire size decreased. While the UV emission corresponds to the near band-edge emission, the green emission peak is commonly referred to as deep-level or trap-state emission. The green transition has been attributed to the singly ionized oxygen vacancy in ZnO and the emission results from the radiative recombination of a photo-generated hole with an electron occupying the oxygen vacancy.[37] The progressive increase of the green emission relative to the UV emission as the wire diameter decreases suggests that there is a greater fraction of oxygen vacancies in the thinner nanowires. We believe a higher surface area to volume ratio for thinner wires might favor a higher level of surface and sub-surface oxygen vacancy under the current reductive environment.[10]

In order to explore the possible stimulated emission from the oriented nanowires, the power-dependent emission has been examined. The samples were optically pumped by the fourth harmonic of a Nd:YAG laser (266 nm, 3 ns pulse width) at room temperature. The pump beam was focused on nanowires at an incidence angle 10° to the symmetric axis of the nanowire. Light emission was collected in the direction normal to the end surface plane (along the symmetric axis) of the nanowires (Fig. 13A). Significantly, in the absence of any fabricated mirrors, we observed lasing action in these ZnO nano-

4. Photoluminescence and Lasing Properties

Photoluminescence spectra of nanowires of different diameters were measured using an He–Cd laser (325 nm) as the excitation source. Figure 12 shows the room-temperature PL spectra of nanowires with an average diameter of 100, 50, and 25 nm. Strong emission at ~380 nm was observed for all nanowires. In addition, we observed that the green emission intensity at ~520 nm increased as the nano-

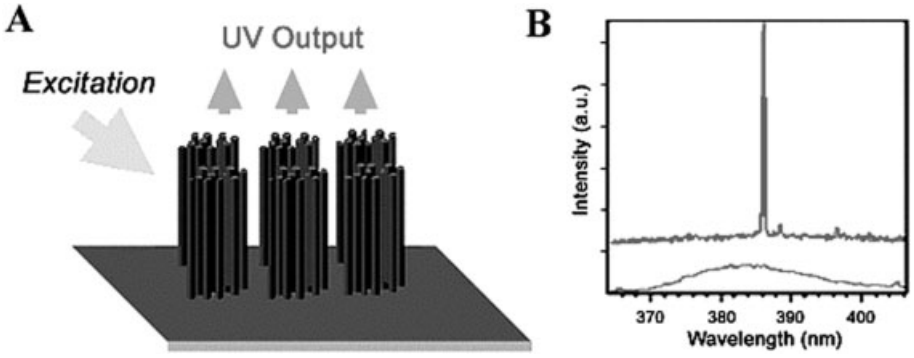

Fig. 13. A) Schematic illustration of the experimental set-up for the power-dependent emission studies. B) Emission spectra from vertical ZnO nanowire arrays on *a*-plane sapphire substrate below and above the lasing threshold. The spectra are offset for easy comparison.

© WILEY-VCH Verlag GmbH, D-69469 Weinheim, 2002
1616-301X/02/0505-0328 $ 17.50+.50/0

ADVANCED FUNCTIONAL MATERIALS

wires. Figure 13B shows the evolution of the emission spectra as we increased the pump power.[7] At low excitation intensity, the spectrum consists of a single broad spontaneous emission (Fig. 13B, bottom trace) peak with a full width at half maximum (FWHM) of approximately 17 nm. This spontaneous emission is 140 meV below the bandgap (3.37 eV) and is generally ascribed to the recombination of excitons through an exciton–exciton collision process where one of the excitons radiatively recombines to generate a photon. As the pump power increases, the emission peak narrows due to the preferential amplification of frequencies close to the maximum of the gain spectrum. When the excitation intensity exceeds a threshold (~40 kW cm^{-2}), sharp peaks emerge in the emission spectrum (Fig. 13B, upper trace). The line widths of these peaks are less than 0.3 nm, which is more than 50 times smaller than the line width of the spontaneous emission peak below the threshold. Above the threshold, the integrated emission intensity increases rapidly with pump power. The narrow line width and the rapid increase of emission intensity indicate that stimulated emission takes place in these nanowires. The observed single or multiple sharp peaks represent different lasing/cavity modes at wavelengths between 370 and 400 nm. It is noted that the lasing threshold is quite low compared with previously reported values for random lasing (~300 kW cm^{-2}) in disordered particles or thin films.

The fact that we observed lasing action in these nanowire arrays without any fabricated mirror prompts us to consider these single-crystalline, well-facetted nanowires as natural resonance cavities (Fig. 14). It is possible that the giant oscillator strength effect, which can occur in high-quality nanowire crystals with dimensions larger than the exciton Bohr radius, but smaller than the optical wavelength, enables excitonic stimulated emission in these nanowire arrays. For II–VI semiconductors, a cleaved edge of the specimen is usually used as a mirror.[38] For our nanowires, one end is the epitaxial interface between the sapphire and ZnO while the other end is the sharp (0001) plane of the ZnO nanocrystals. Both can serve as good laser cavity mirrors considering the refractive indexes for sapphire, ZnO, and air are 1.8, 2.45, and 1, respectively. This natural cavity/waveguide formation in nanowires suggests a simple chemical approach to form a nanowire laser cavity without cleavage and etching. In fact, when multiple lasing modes were observed for these nanowires, the observed mode spacing was about 6 nm for ~5 μm long wires, which agrees well quantitatively with the calculated spacing between adjacent resonance frequencies $\upsilon_F = c/2nl$, where υ_F is the emission mode spacing, c is the speed of light, n is the refractive index, and l is the resonance cavity length.

To further validate this proposed model, isolated nanowire lasing experiments were carried out, as there is some argument that the lasing might originate from the amplified stimulated emission based on random scattering. Figure 10 shows the SEM image of the isolated ZnO nanowires used in this study. The average spacing between these wires is about 2–3 μm, so it is almost impossible to amplify the stimulated light emission by scattering in such a sparsely distributed nanowire array. Figure 15 shows a lasing spectrum from these isolated nanowires, which is similar to those obtained for dense arrays. This suggests that the lasing indeed originated from a single nanowire, not by amplification of scattering in the dense nanowire array.

Furthermore, single nanowire lasing experiments by near-field scanning optical microscopy (NSOM) were also carried out to demonstrate the lasing mechanism.[36] In order to be imaged with NSOM, the wires were removed from the sapphire growth substrate by sonication and dispersed onto a quartz substrate by drop casting an ethanol–nanowire mixture. The nanowires were excited with short pulses (<300 fs) of 4.35 eV photons (285 nm) in order to induce photoluminescence (PL) and lasing (Fig. 16). The nanowire emission was collected by a

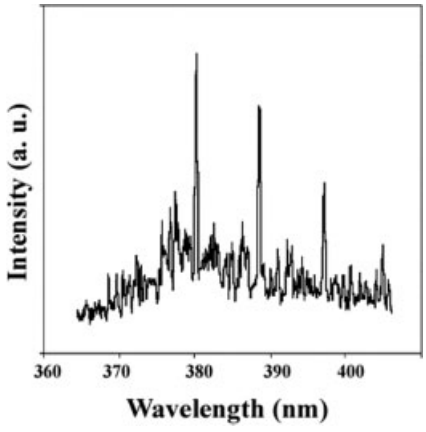

Fig. 15. Emission spectrum above the lasing threshold collected from vertical ZnO nanowire arrays of low areal density on *a*-plane sapphire substrate.

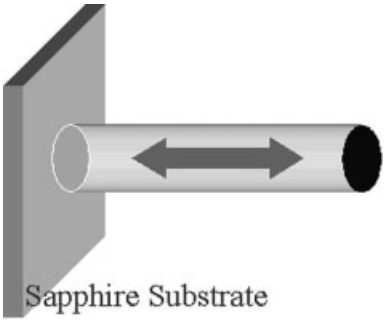

Fig. 14. Schematic illustration of a nanowire as a resonance cavity with two naturally faceted hexagonal end faces acting as reflecting mirrors.

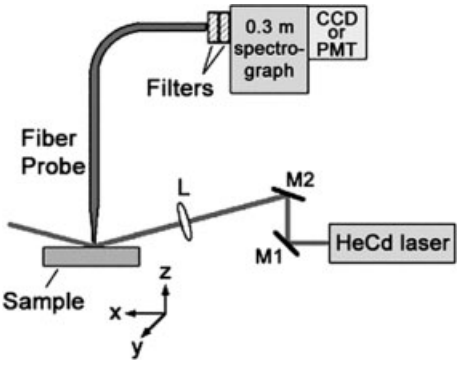

Fig. 16. Illustration of NSOM set-up for power-dependent emission studies on a single ZnO nanowire.

 © WILEY-VCH Verlag GmbH, D-69469 Weinheim, 2002 1616-301X/02/0505-0329 $ 17.50+.50/0

chemically etched fiber optic probe held in constant-gap mode by the feedback electronics of the NSOM. Figure 17 shows the spatially resolved emission collected in a 70 nm wide spectral band centered at 400 nm. Strong PL emission can be clearly seen at the end of the nanowire, while only very weak emission was detected from the side surfaces of the nanowire. Significant peak narrowing is observed for the emission emanating from the end of the nanowire. The power dependence of the nanowire emission exhibits a clear threshold near the excitation intensity of approximately 120 kW cm^{-2} (using a sub-picosecond laser pulse width). This threshold is higher than that observed from bulk wires, although it is of the same order of magnitude. The single nanolasers dispersed onto the quartz substrate are likely to exhibit a higher threshold than those attached to the growth substrate, considering the possible damage to the end faces that occurs during sample preparation. Nanowire coupling could also contribute to a lowering of the lasing threshold for the nanowire arrays.

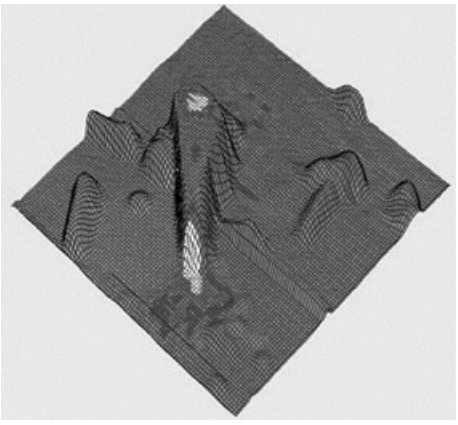

Fig. 17. Spatially resolved NSOM emission image collected on a single ZnO nanowire in a 70 nm wide spectral band centered at 400 nm.

In addition, lifetime measurements show that the radiative recombination of the excitons is a superposition of a fast and a slow process with time constants of about 70 ps and 350 ps, respectively.[7,10] The luminescence lifetime is mainly determined by the concentration of defects, which trap the electrons and/or holes and eventually cause their non-radiative recombination. Although the exact origin of the luminescence decay remains unclear at this stage, the long lifetime measured for these wires demonstrates the high crystal quality achieved with the nanowire growth process. It also accounts in part for the low laser threshold of the wire.

5. Conclusion and Outlook

In summary, we successfully synthesized ZnO nanowires via a VLS growth mechanism using Au as the solvent. Orientational control of the nanowires was achieved by epitaxial growth on sapphire substrates. By controlling the pattern of the Au thin film, we succeeded in growing ordered ZnO nanowire arrays. ZnO nanowires of different sizes and densities were grown by varying the thickness of the Au layers or the diameter of the Au clusters.

Room-temperature photoluminescence of the nanowires shows the near band-edge emission and the deep level emission. An enhanced deep-level emission for thinner nanowires has been observed and attributed to their larger surface area. Furthermore, room-temperature ultraviolet lasing in well-oriented vertical ZnO nanowires with a lasing threshold of 40 kW cm^{-2} was demonstrated. Grown in the <0001> direction, these single-crystalline, well-facetted nanowires form natural laser resonance cavities. This proposed lasing model was further validated by controlled lasing experiments on isolated ZnO nanowires and single-nanowire lasing experiments by NSOM.

It should be emphasized that the concept of using well-cleaved nanowires as natural optical cavities should be applicable to many other different semiconductor systems such as GaN and CdSe. Our results obtained on the ZnO nanowire system suggest the feasibility of nanoscale surface-emitting lasers operating at ultraviolet or other wavelengths when the material of the nanowire cavity is altered. In addition, by creating p–n junctions in these individual nanowires, one should be able to test the possibility of making electron ejection UV/blue lasers out of individual nanowires. Such miniaturized nanowire nanolasers will find applications in nanophotonics and microanalysis.

Received: February 6, 2002

[1] J. Hu, T. W. Odom, C. M. Lieber, *Acc. Chem. Res.* **1999**, *32*, 435.
[2] Y. Wu, H. Yan, P. Yang, *Chem. Eur. J.* **2002**, *8*, 1260.
[3] P. Yang, Y. Wu, R. Fan, *Int. J. Nanosci.* **2002**, in press.
[4] E. W. Wang, P. E. Sheehan, C. M. Lieber, *Science* **1997**, *277*, 1971.
[5] J. D. Holmes, K. P. Johnston, R. C. Doty, B. A. Korgel, *Science* **2000**, *287*, 1471.
[6] L. D. Hicks, M. S. Dresselhaus, *Phys. Rev. B* **1996**, *47*, 16 631.
[7] M. Huang, S. Mao, H. Feick, H. Yan, Y. Wu, H. Kind, E. Weber, R. Russo, P. Yang, *Science* **2001**, *292*, 1897.
[8] a) Y. Wu, P. Yang, *Chem. Mater.* **2000**, *12*, 605. b) Y. Wu, B. Messer, P. Yang, *Adv. Mater.* **2001**, *13*, 1487. c) Y. Wu, P. Yang, *J. Am. Chem. Soc.* **2001**, *123*, 3165.
[9] C.-C. Chen, C.-C. Yeh, *Adv. Mater.* **2000**, *12*, 738.
[10] M. H. Huang, Y. Wu, H. Feick, E. Weber, P. Yang, *Adv. Mater.* **2001**, *13*, 113.
[11] M. Yazawa, M. Koguchi, A. Muto, M. Ozawa, K. Hiruma, *Appl. Phys. Lett.* **1992**, *61*, 2051.
[12] Y. Wu, R. Fan, P. Yang, *Nano Lett.* **2002**, *2*, 83.
[13] Y. C. Choi, W. S. Kim, Y. S. Park, S. M. Lee, D. J. Bae, Y. H. Lee, G.-S. Park, W. B. Choi, N. S. Lee, J. M. Kim, *Adv. Mater.* **2000**, *12*, 746.
[14] a) X. F. Duan, C. M. Lieber, *Adv. Mater.* **2000**, *12*, 298. b) A. M. Morales, C. M. Lieber, *Science* **1998**, *279*, 208.
[15] T. J. Trentler, K. M. Hickman, S. C. Goel, A. M. Viano, P. C. Gibbons, W. E. Buhro, *Science* **1995**, *270*, 1791.
[16] a) M. H. Huang, A. Choudrey, P. Yang, *Chem. Commun.* **2000**, *12*, 1603. b) J. Zhu, S. Fan, *J. Mater. Res.* **1999**, *14*, 1175.
[17] Y. Li, G. W. Meng, L. D. Zhang, F. Philipp, *Appl. Phys. Lett.* **2000**, *76*, 2011.
[18] P. Yang, C. M. Lieber, *Science* **1996**, *273*, 1836.
[19] Z. W. Pan, Z. R. Dai, Z. L. Wang, *Science* **2001**, *291*, 1947.
[20] D. A. Gaul, W. S. Rees, Jr. *Adv. Mater.* **2000**, *12*, 935.
[21] M. A. Hasse, J. Que, J. M. De Puydt, H. Cheng, *Appl. Phys. Lett.* **1991**, *59*, 1272.
[22] S. Nakamura, M. Senoh, S. Nagahama, N. Iwasa, T. Yamada, T. Matsushita, H. Kiyoku, Y. Sugimoto, *Jpn. J. Appl. Phys.* **1996**, *35*, L74.
[23] H. Cao, J. Y. Xu, D. Z. Zhang, S. H. Chang, S. T. Ho, E. W. Seeling, X. Liu, R. P. H. Chang, *Phys. Rev. Lett.* **2000**, *84*, 5584.
[24] D. M. Bagnall, Y. F. Chen, Z. Zhu, T. Yao, S. Koyama, M. Y. Shen, T. Goto, *Appl. Phys. Lett.* **1997**, *70*, 2230.

 © WILEY-VCH Verlag GmbH, D-69469 Weinheim, 2002 1616-301X/02/0505-0330 $ 17.50+.50/0

[25] P. Yu, Z. K. Tang, G. K. L. Wong, M. Kawasaki, A. Ohtomo, H. Koinuma, Y. Segawa, *J. Cryst. Growth* **1998**, *184/185*, 601.
[26] C. Klingshirn, *J. Cryst. Growth* **1992**, *117*, 753.
[27] Y. Kayamura, *Phys. Rev. B* **1988**, *38*, 9797.
[28] W. Wegscheider, L. N. Pfeiffer, M. M. Dignam, A. Pinczuk, W. K. West, S. L. McCall, R. Hull, *Phys. Rev. Lett*. **1993**, *71*, 4071.
[29] D. Mehus, D. Evans, *Laser Focus World* **1995**, *31*, 117.
[30] J. F. Wang, M. S. Gudiksen, X. F. Duan, Y. Cui, C. M. Lieber, *Science* **2001**, *293*, 1455.
[31] K. Hiruma, M. Yazawa, T. Katsuyama, K. Ogawa, K. Haraguchi, M. Koguchi, H. Kakibayashi, *J. Appl. Phys.* **1995**, *77*, 447.
[32] V. I. Klimov, A. A. Mikhailovsky, S. Xu, A. Malko, J. A. Hollingsworth, C. A. Leatherdale, H. J. Eisler, M. G. Bawendi, *Science* **2000**, *290*, 314.
[33] L. Pavesi, L. D. Negro, C. Mazzoleni, G. Granzo, F. Priolo, *Nature* **2000**, *408*, 440.
[34] H. Kind, H. Yan, M. Law, B. Messer, P. Yang, *Adv. Mater*. **2002**, *14*, 158.
[35] J. C. Johnson, H. Yan, R. D. Schaller, P. B. Peterson, P. Yang, R. J. Saykally, *Nano Lett*. **2002**, *2*, 279.
[36] J. Johnson, H. Yan, R. Schaller, L. Haber, R. Saykally, P. Yang, *J. Phys. Chem*. *B* **2001**, *105*, 11 387.
[37] K. Vanheusden, W. L. Warren, C. H. Seager, D. R. Tallant, J. A. Voigt, B. E. Gnage, *J. Appl. Phys.* **1996**, *79*, 7983.
[38] *Fundamentals of Photonics* (Eds: B. E. A. Saleh, M. C. Teich), Wiley, New York **1991**.

 © WILEY-VCH Verlag GmbH, D-69469 Weinheim, 2002 1616-301X/02/0505-0331 $ 17.50+.50/0